

1
2
3
4
5
6
7
8
9
10
11
12
13
14
15
16
17
18
19
20
21
22
23
24
25
26
27
28
29
30
31
32
33
34
35
36
37
38
39
40
41
42
43
44
45
46
47
48
49
50
51
52
53
54
55
56
57
58
59
60
61
62
63
64
65

Evaluation of measurement method for carbon fiber length using an optical image scanner

Mariko Terada ^a, Atsuhiko Yamanaka ^a, Yukitane Kimoto ^b, Daisuke Shimamoto ^c, Yuji Hotta ^{a,c} and Takashi Ishikawa ^a

^a *National Composites Center Japan, Nagoya University, Furo-cho, Chikusa-ku, Nagoya, 464-8603, Japan, +81-52-789-2562, terada@ncc.engg.nagoya-u.ac.jp*

^b *Automotive Center, Toray Industries, Inc., 9-1, Oe-cho, Minato-ku, Nagoya, 455-8502, Japan, +81-52-613-5911, Yukitane_Kimoto@nts.toray.co.jp*

^c *National Institute of Advanced Industrial Science and Technology, Shimoshidami, Moriyama-ku, Nagoya, 463-8560, Japan, +81-52-736-7153, y-hotta@aist.go.jp*

Evaluation of the measurement method for carbon fiber length using an optical image scanner

Fiber length and its distribution are important factors to determine the mechanical properties of discontinuous carbon fiber reinforced composites. For the efficient and easy measurement of fiber length, an optical image scanner was introduced into the measurement procedure. The scan image allowed to measure approximately 25000 carbon fibers. The measured values (L_{sc}) were evaluated by comparison with reference values (L_{mi}) obtained by using an optical microscope. L_{sc} were dependent on the angle between fiber and sub-scanning direction. Furthermore, the relative errors between L_{sc} and L_{mi} were less than 2.5 % in case that L_{mi} were 0.226 mm or more. The sample standard deviations of L_{sc} were approximately constant and their values were ca. 0.010 mm. Therefore, it was found that the relative error of measurement value derived from the scan image was dependent on the measured fiber length.

Keywords: discontinuous carbon fiber; scanner; fiber length distribution; measurement errors

1. Introduction

Recently, carbon fiber reinforced plastics (CFRPs) have been attracting attention for use in aircraft, aerospace, automobile, and other industries because of their light weight and good mechanical properties. Compared to metallic materials, CFRP has various advantages, such as high strength to weight ratio, good corrosion resistance, and excellent fatigue tolerance [1–5]. Moreover, CFRPs fabricated by discontinuous carbon fibers have been used for automobile components because of their good productivity and low manufacturing cost. Injection molding has been used effectively as a CFRP manufacturing process. However, composites fabricated by injection molding have a wide-range fiber length distribution because of fiber breakage caused by the processing. Fiber length distribution is a factor dominating the mechanical properties of the

1 composites, along with fiber content, fiber orientation distribution, and interface adhesion
2 between the fiber and the matrix [6–9]. Fiber length distribution has often been explained
3 with relevance to critical fiber length. The average fiber length has also been used as an
4 index. For example, it has been reported that the average length of the fibers comprising
5 carbon fiber reinforced polypropylenes is reflected by their impact resistance [10].
6 Therefore, it is important to evaluate the fiber length and distribution for the development
7 of composites with excellent mechanical properties.
8
9

10
11
12
13
14
15
16
17 Generally, fiber length and its distribution can be estimated by microscopic
18 images, but in this case, there is a strict trade-off between magnification and observation
19 area. It is known that a carbon fiber has a diameter less than 10 μm and its aspect ratio
20 can vary from less than one to several thousands. Therefore, suitable magnification of
21 the diameter does not always correspond to sufficient observation area. Moreover, the
22 number of samples counted in an observation area is limited by the dimension. Hence,
23 measurement procedures are often required to be repeated to collect a sufficient number
24 of samples for the evaluation of fiber length distribution by microscopic images. Lunt
25 and Shortall pointed out that a specimen with an extremely wide fiber length
26 distribution requires a sample count of approximately 2000 for accurate characterization
27 of the distribution [7]. From this point of view, X-ray computed tomography (CT)
28 scanning is a powerful technique for investigating the fiber length and its distribution in
29 composites [11]. However, the apparatus is expensive, and the measurement time is
30 quite long. Furthermore, because the carbon fiber is thin, a high resolution is required.
31 Therefore, the measurement area in X-ray CT scanning may be too narrow for the
32 observation of a carbon fiber. In other words, the abovementioned trade-off between
33 magnification and observation area is unavoidable even in the case of X-ray CT
34 scanning. In addition, carbon fibers with density similar to that of matrix resins are
35
36
37
38
39
40
41
42
43
44
45
46
47
48
49
50
51
52
53
54
55
56
57
58
59
60
61
62
63
64
65

1 difficult to detect. Thus, it is necessary to develop another method for the rapid
2 measurement of fiber length and its distribution in a large area.
3

4 Optical image scanning can be a possible solution to this problem. The upper
5 limit of output image size for a typical commercial optical image scanner is above 100 M
6 pixel, meaning that a scan image of 2400 dpi can cover an area of 10000 mm². A fiber
7 length analyzer with a high-resolution optical image scanner has been commercialized
8 [12,13]. However, the accuracy and precision of the fiber length measured from these
9 scanned images have not been investigated in detail.
10

11 In this paper, we report a method for the measurement of fiber length using an
12 optical image scanner and discuss the accuracy and precision of the measured values.
13

14 **2. Experiments**

15 ***Materials***

16 All chemicals and materials were used as received without further purification. Carbon
17 fiber tow (TORAYCA T700) was purchased from Toray Industries, Inc. Polyvinyl
18 alcohol (PVA: PVA-217SB, Kuraray CO., LTD.) was used as the dispersant.
19

20 ***Preparation of sample sheet for measurement***

21 The carbon fiber tow was cut into 10 mm pieces, which were burned at 440 °C for 10 h
22 in an electric furnace (FO810, Yamato Scientific Co., Ltd.). The fiber bundle was added
23 to 100 mL of 8 wt% PVA aqueous solution, and the suspension was stirred using a
24 magnetic stirrer to disperse the carbon fibers homogeneously. Then, 20 ml of the
25 suspension was cast on a plastic tray with inner dimensions of 125 mm × 200 mm. The
26 casted suspension was dried at 50 °C in air to prepare a sample sheet. The sample sheet
27 was removed from the tray.
28
29
30
31
32
33
34
35
36
37
38
39
40
41
42
43
44
45
46
47
48
49
50
51
52
53
54
55
56
57
58
59
60
61
62
63
64
65

1
2
3
4 ***Measurement of fiber length distribution***
5

6 The sample sheet was scanned by an optical image scanner (GT-X830, SEIKO EPSON
7 Co.) with 2400 dpi resolution. A scanned image with a gradation of 256 was obtained
8 by the scanner. In order to abstract the fibers, the scanned image was binarized, where
9 gradations from 0 to 95 were shown as black and those from 96 to 255 were shown as
10 white. For proper image recognition, the abstracted area was dilated with 2 pixels,
11 namely if abstracted area was a circle with a radius of 10 pixels, this radius was extend
12 to be 12 pixels. The length of the abstracted line was measured by the “Needle Shape
13 Particle Measurement” function of an image analysis software (WinRoof, Mitani CO.
14 Ltd.), which is a command for measuring the length of needle-like materials. The
15 purpose of this study is to characterize the CF length measured using this scanner
16 method. According to the algorithm of this software, the fiber length is measured from
17 the binary image of a needle fiber. The algorithm is not provided in the section because
18 the software is commercially available. As the measurement parameters, the Min
19 Length and Max Width were set to 12 pixels. In order to offset the dilation, 4 pixels
20 were subtracted from the measured results. Hence, the equivalent lower limit of the
21 measured length was 8 pixels. According to the scan resolution, 1 pixel in the image
22 was counted as 0.01058 mm.
23
24
25
26
27
28
29
30
31
32
33
34
35
36
37
38
39
40
41
42
43
44
45
46
47
48
49
50
51

52 ***Determination of fiber length from the scanned image***
53

54 The sample sheet was scanned at a resolution of 2400 dpi while rotating until
55 the rotation angle reached 180°. In this work, 10 scanned images with different rotation
56 angles were obtained. From each scanned image, six fibers with different lengths were
57
58
59
60
61
62
63
64
65

1 selected as evaluation objects. Figure 1 shows one of the six fibers with the 10 rotation
2 angles. The lengths of the evaluation objects were measured by the above-described
3 method. However, the Min Length was set to 3 pixels in this case. The fiber lengths
4 estimated from this procedure were defined as L_{sc} .
5
6
7
8
9

10 For analysis of L_{sc} , measured values of the evaluation objects obtained using
11 an optical microscope (DSX500, Olympus Corporation) and by manual measurement
12 were used. These measured values were defined as L_{mi} .
13
14
15
16
17

18 **3. Results**

19 ***Measurement of fiber length distribution***

20 Figure 2 shows a scanned image of the sample sheet. A large area of the fibers was
21 clearly observed in the image. Figure 3 shows fiber length distribution derived from the
22 sample sheet in Figure 2. Approximately 25000 fibers measured from the scanned
23 image. Many short fibers could be detected in the scanned image, indicating that most
24 original fibers broke during the sample preparation. Moreover, a small peak appeared at
25 a fiber length of 10 mm, indicating that some of the original fibers did not break during
26 the sample preparation process.
27
28
29
30
31
32
33
34
35
36
37
38
39
40
41
42

43 ***Determination of fiber length from the scanned image***

44 Figure 4 is a part of Figure 2. In this image, the fiber widths ranged from 3 to 5
45 pixels. According to the resolution, these pixel values were estimated to be 30 to 50 μm .
46 Considering that the diameter of the T700 carbon fiber is 7 μm , the estimated values
47 were found to be too large. Therefore, it was found that the diameter of the carbon fiber
48
49
50
51
52
53
54
55
56
57
58
59
60
61
62
63
64
65

measured from the scanned image was larger than the actual diameter.

Considering this phenomenon, we investigated the accuracy and precision of the measured fiber length (L_{sc}). L_{sc} was evaluated by comparison with L_{mi} . The mean carbon fiber lengths $\langle L_{sc} \rangle$, standard deviations of L_{sc} and relative errors (E_m) of six fibers with different lengths are shown in Table 1. $\langle L_{sc} \rangle$ was estimated from L_{sc} of 10 scanned images at different rotation angles. For example, for a fiber with L_{mi} of 1.334 mm, $\langle L_{sc} \rangle$ was estimated by the fiber images in Figure 1. Herein, we assumed that the orientation of the carbon fibers on the sample sheets was random based on our observation of Figure 2, and $\langle L_{sc} \rangle$ was used as an index for the evaluation of measurement errors. The errors (E_a) and relative errors (E_m) of the measured values are represented as follows:

$$E_a = \langle L_{sc} \rangle - L_{mi} \quad (1)$$

$$E_m = (\langle L_{sc} \rangle - L_{mi})/L_{mi} \quad (2)$$

The carbon fiber of 0.040 mm cannot be detected from the scan images. This result suggests that the lower limit of detection for the fiber length under these conditions is a value between 0.040 mm and 0.067 mm.

As shown in Table 1, the relative measurement error was within 2.5% for a carbon fiber length of 0.226 mm or greater, whereas the error was estimated to be 10% or more for fairly short carbon fibers, i.e., length lesser than 0.100 mm. On the other

1 hand, the standard deviations of L_{SC} were constant at approximately 0.010 mm
2 regardless of the L_{mi} value. In this study, scanned images with a resolution of 2400
3 dpi were used, meaning that the standard deviations of L_{SC} were about 1 pixel. This
4 measurement precision is very high as an image analysis.
5
6
7
8
9

10 Figure 5 shows a top view photograph of the scanner used in this work. For an
11 optical image scanner, the short and long sides on a document table are represented as
12 the main-scanning and sub-scanning directions, respectively. In this study, the angle
13 between the long side on the document table and a carbon fiber was defined as θ , as
14 shown in Figure 5. Therefore, the value of θ could range from 0° to 90° . Figure 6
15 represents the relationship between E_a and θ for L_{mi} values of 1.334, 0.595, 0.226,
16 0.099, and 0.067 mm. E_a decreased with increasing θ . When a fiber was parallel to the
17 sub-scanning direction, the measured fiber length tended to be greater than that
18 estimated from the optical microscope image. Hence, the fiber lengths estimated from
19 the scanned images were dependent on the angle between the fiber and the sub-scanning
20 direction.
21
22
23
24
25
26
27
28
29
30
31
32
33
34
35
36
37
38
39
40
41

42 **4. Discussion**

43 In this study, we use an optical image scanner with a charge-coupled device (CCD), as
44 shown in Figure 7. As shown in Figure 6, the values of L_{SC} depend on θ . It has been
45 reported that the shadow of an object appears in the sub-scanning direction [14]. Thus,
46 the dependence between L_{SC} and θ is caused by the shadow in the sub-scanning
47 direction. In the case of an optical image scanner, the light-source-and-mirror units are
48 set at the front and back in the sub-scanning direction, as shown in Figure 7. Therefore,
49 the shadow appears on the front or back side in the sub-scanning direction. Figure 8
50
51
52
53
54
55
56
57
58
59
60
61
62
63
64
65

1 shows schematic diagrams of a carbon fiber during scanning. The shadow of a carbon
2 fiber is caused by scanning at various θ values. Assuming that length of the shadow in
3 sub-scanning direction is constant, influence of this length on measured fiber length
4 becomes greater as $\cos \theta$ rises.
5
6
7
8
9

10 Figure 9 shows that the coefficient of variation of L_{sc} (CV) is proportional to
11 the inverse of L_{mi} and $\langle L_{sc} \rangle$ ($1/L$). This implies that the measurement precision is
12 inversely proportional to the object size. Therefore, an acceptable lower limit can be
13 estimated from the inversely proportional relationship between the fiber length and the
14 required precision.
15
16
17
18
19
20
21
22
23
24
25
26
27

28 **5. Conclusion**

29 In this study, we investigated a method for the measurement of carbon fiber
30 length using an optical image scanner. The optical image scanner provided a large
31 measurement area, and approximately 25000 fibers were measurable in the scanned
32 image. On the other hand, the fiber length measured from the scanned image was
33 slightly different from that estimated by an optical microscope. The following
34 conclusions could be drawn.
35
36
37
38
39
40
41
42
43
44
45

- 46 1) The measurement error was within 2.5% for carbon fiber lengths 0.226 mm or
47 greater, whereas the error was higher than 10% for fairly short carbon fibers
48 (lengths smaller than 0.100 mm).
49
50
51
52
53
- 54 2) The fiber length estimated by the scanned image was dependent on the angle
55 between the fiber and the sub-scanning direction of the scanner.
56
57
58
59
60
61
62
63
64
65

1 An important consequence is that the error in the measured value derived from the
2 scanned image depends on the measured object size, and the acceptable lower
3 measurement limit can be estimated by the dependence of the error on the fiber length.
4
5 The carbon fiber length and its distribution derived from an optically scanned image are
6
7 valid within an appropriate measurement range.
8
9

10
11 Furthermore, optical image scanning is an effective technique to measure carbon
12 fiber length and its distribution without the need for expensive instruments such as X-
13 ray CT scanners. Therefore, this method may be an alternative approach to measure
14 carbon fiber length and its distribution.
15
16
17
18
19
20
21
22
23

24 Acknowledgement

25 The authors acknowledge the support from the future-pioneering program commissioned by
26 New Energy and Industrial Technology Development Organization (NEDO) for the present
27 study.
28
29
30
31
32
33

34 References

- 35
36 [1] Ashrafi B, Guan J, Mirjalili V, et al. Enhancement of mechanical performance of
37 epoxy/carbon fiber laminate composites using single-walled carbon nanotubes.
38 Compos. Sci. Technol. 2011;71:1569–1578.
39
40 [2] Khan SU, Kim JK. Improved interlaminar shear properties of multiscale carbon
41 fiber composites with bucky paper interleaves made from carbon nanofibers.
42 Carbon N. Y. 2012;50:5265–5277.
43
44 [3] Rezaei F, Yunus R, Ibrahim N a. Effect of fiber length on thermomechanical
45 properties of short carbon fiber reinforced polypropylene composites. Mater.
46 Des. 2009;30:260–263.
47
48 [4] Karnik SR, Gaitonde VN, Rubio JC, et al. Delamination analysis in high speed
49 drilling of carbon fiber reinforced plastics (CFRP) using artificial neural network
50 model. Mater. Des. 2008;29:1768–1776.
51
52
53
54
55
56
57
58
59
60
61
62
63
64
65

- 1
2
3
4
5
6
7
8
9
10
11
12
13
14
15
16
17
18
19
20
21
22
23
24
25
26
27
28
29
30
31
32
33
34
35
36
37
38
39
40
41
42
43
44
45
46
47
48
49
50
51
52
53
54
55
56
57
58
59
60
61
62
63
64
65
- [5] Davis DC, Wilkerson JW, Zhu J, et al. A strategy for improving mechanical properties of a fiber reinforced epoxy composite using functionalized carbon nanotubes. *Compos. Sci. Technol.* 2011;71:1089–1097.
 - [6] Kelly A, Tyson WR. Tensile properties of fibre-reinforced metals: Copper/tungsten and copper/molybdenum. *J. Mech. Phys. Solids.* 1965;13:329–350.
 - [7] Lunt JM, Shortall JB. The effect of extrusion compounding on fibre degradation and dtrength properties in short glass-fibre-reinforced nylon 6.6. *Plast. Rubber Process.* 1979. p. 108–111.
 - [8] Koyanagi J, Ogihara S, Nakatani H, et al. Mechanical properties of fiber/matrix interface in polymer matrix composites. *Adv. Compos. Mater.* 2014;23:551–570.
 - [9] Fu SY, Lauke B. Effects of fiber length and fiber orientation distributions on the tensile strength of short-fiber-reinforced polymers. *Compos. Sci. Technol.* 1996;56:1179–1190.
 - [10] Hirano N, Muramatsu H, Inoue T. Study of fiber length and fiber-matrix adhesion in carbon-fiber-reinforced polypropylenes. *Adv. Compos. Mater.* 2014;23:151–161.
 - [11] Alemdar A, Zhang H, Sain M, et al. Determination of Fiber Size Distributions of Injection Moulded Polypropylene/Natural Fibers Using X-ray Microtomography. *Adv. Eng. Mater.* [Internet]. 2008;10:126–130. Available from: <http://doi.wiley.com/10.1002/adem.200700232>.
 - [12] Müssig J, Schmid HG. Quality Control of Fibers Along the Value Added Chain by Using Scanning Technique - from Fibers to the Final Product. *Microsc. Microanal.* [Internet]. 2004;10:1332–1333. Available from: <https://www.cambridge.org/core/article/quality-control-of-fibers-along-the-value-added-chain-by-using-scanning-technique-from-fibers-to-the-final-product/51F965E8072A062F0C4F8F9F253A46B9>.
 - [13] Fischer H, Schmid HG. Quality control for recycled carbon fibres. *Kunststoffe Int.* 2013;68–71.
 - [14] Sudo T. Observation of rock flagments with personal computer and scanner. *Chishitsu News.* 2002;46–52.

1
2
3
4
5
6
7
8
9
10
11
12
13
14
15
16
17
18
19
20
21
22
23
24
25
26
27
28
29
30
31
32
33
34
35
36
37
38
39
40
41
42
43
44
45
46
47
48
49
50
51
52
53
54
55
56
57
58
59
60
61
62
63
64
65

Table.1 Mean value of the measurements ($\langle L_{sc} \rangle$), their sample standard deviation and their errors.

L_{mi} (mm)	$\langle L_{sc} \rangle$ (mm)	$\sqrt{\frac{1}{10} \sum_{i=1}^{10} (L_{sc} - \langle L_{sc} \rangle)^2}$ (mm)	$\frac{\langle L_{sc} \rangle - L_{mi}}{L_{mi}}$
1.334	1.357	0.014	0.017
0.595	0.591	0.009	-0.006
0.226	0.231	0.010	0.021
0.099	0.082	0.011	-0.172
0.067	0.060	0.012	-0.102
0.040	-	-	-

Figure 1. Scan image of sample for the comparison between L_{sc} and L_{mi} (indicated blue characters)

Figure 2. Whole scan image of the sheet.

Figure 3. Fiber length distribution counted from scan image of the sheet adopting 2400 dpi resolution.

Figure 4. A part of scan image of the sheet shown in Figure 3.

Figure 5. Top view of the scanner used in this work. θ is angle between a fiber and sub-scanning direction.

Figure 6. Relationship between θ and measurement errors of the fiber length (E_a) that corresponding each standard fiber length (L_{mi}).

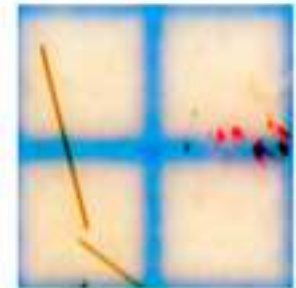
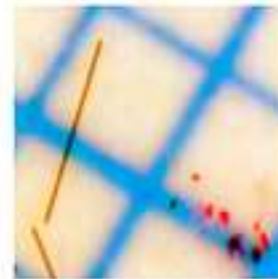
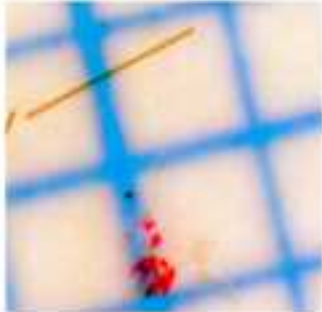
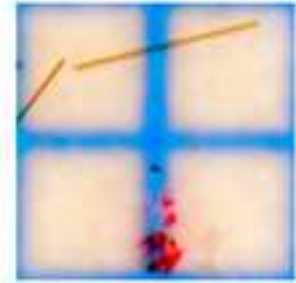
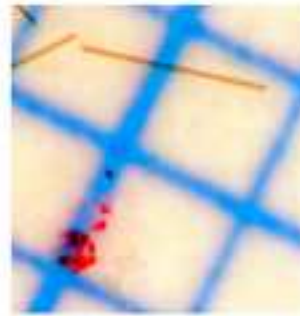
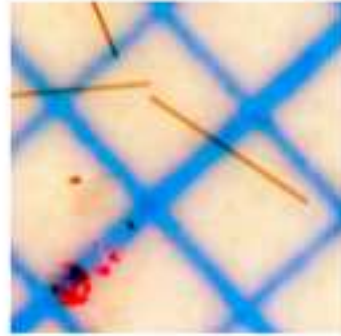
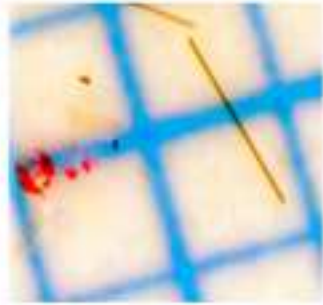
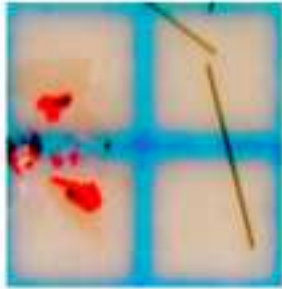
Figure 7. Schematic diagram of mechanism of a CCD scanner [14].

Figure 8. Schematic diagram of carbon fiber and its shadow caused by scanning.

Figure 9. Relationship between coefficient of variation of L_{sc} and inverse of L_{mi} and $\langle L_{sc} \rangle$.

1
2
3
4
5
6
7
8
9
10
11
12
13
14
15
16
17
18
19
20
21
22
23
24
25
26
27
28
29
30
31
32
33
34
35
36
37
38
39
40
41
42
43
44
45
46
47
48
49
50
51
52
53
54
55
56
57
58
59
60
61
62
63
64
65

1334 μm



1mm

